ChemComm
Chemical Communications

Accepted Manuscript

This article can be cited before page numbers have been issued, to do this please use: L. Yang, B. An, X. Yin and F. Li, *Chem. Commun.*, 2020, DOI: 10.1039/D0CC01821J.

ROYAL SOCIETY OF CHEMISTRY

rsc.li/chemcomm

View Article Online
DOI: 10.1039/D0CC01821J

COMMUNICATION

Competitive coordination-based immobilization-free electrochemical biosensor for highly sensitive detection of arsenic(V) using CeO_2–DNA nanoprobe

Received 00th January 20xx,
Accepted 00th January 20xx

DOI: 10.1039/x0xx00000x

Limin Yang, Bin An, Xuehan Yin and Feng Li*

We developed a competitive coordination-based immobilization-free electrochemical biosensor for highly sensitive and selective detection of arsenic(V) using CeO_2–DNA nanoprobe, which effectively circumvented complicated modification procedures and successfully achieved arsenic(V) determination in natural water samples.

Arsenic is one of the most important poisonous elements among various heavy metals.[1] Arsenic contamination in natural water has become a severe worldwide threat to human health and ecological systems.[2] Growing evidence demonstrated that chronic exposure to arsenic can cause numerous human diseases, such as skin lesions, cancer, and other disorders.[3] In drinking water, the dominant compositions of arsenic are inorganic arsenic, including As(III) (arsenite) and As(V) (arsenate), which are more toxic than organic arsenic. In oxygen-rich environments, As(V) is a predominant species and it exits as As(V) anions ($H_2AsO_4^-$ and $HAsO_4^{2-}$) under neutral conditions.[4] Many studies show that As(V) could disturb the biological processes by substituting phosphate.[5] When taken up by the cells with a high dosage, As(V) not only changed the characteristics of the membrane but also generated adenosine diphosphate (ADP)-As(V), strongly hindering the conversion of ATP to ADP.[6] Noteworthily, As(V) can cause the generation of superoxide in living cells, which is closely correlated with many physiological and pathological processes.[7] As a consequence, it is of crucial importance to explore simple, sensitive and effective strategies for specifically detecting the level of As(V) in real samples.

Considering the high toxicity of arsenic, the World Health Organization and Environmental Protection Agency have set an acceptable arsenic concentration in drinking water of 10 ppb.[8] To date, some conventional analytical techniques have been exploited to quantify arsenic in water, such as inductively coupled plasma mass spectrometry (ICPMS), atomic absorption spectrometry (AAS), and atomic fluorescence spectrometry (AFS).[9–12] Although these techniques are highly accurate and sensitive, several major limitations including expensive equipment, high operating costs, tedious sample preparation, and long measurement time still exist. Recently, considerable efforts have been devoted to developing new methods for the determination of arsenic, including luminescence, surface-enhanced Raman scattering, fluorescence, colorimetric, and electrochemical sensing protocols.[13–18] Among various approaches, electrochemical methods have gained more intensive consideration for the reliable detection of arsenic due to their simple instrument, easy operation, miniaturizability, low cost, fast response time, and portability.[19] Thus, several well-known electrochemical methods for arsenic assay have been proposed, such as anodic stripping voltammetry and differential pulse voltammetric.[20,21] To achieve the desired sensitivity and selectivity, efficient nanomaterials with outstanding catalytic ability toward arsenic were usually modified on the working electrode surface, such as noble metal, bimetallic, metal oxides, nano biomolecules, and carbon nanomaterials.[22-24] However, most of these electroanalysis sensing strategies were carried out under acidic conditions, which were not suitable for accurately detecting arsenic in natural water samples. In the meantime, some metal oxide nanomaterials may be unstable in acidic media. Furthermore, several intrinsic shortcomings of the nanomaterials in terms of multiple preparation processes, high costs and harsh synthetic conditions are difficult to overcome. By directly immobilizing DNA aptamers instead of nanomaterials on the screen-printed carbon electrode to sensitively detect As(III) was also successfully realized.[25] Unfortunately, all these conventional electrochemical arsenic assays inevitably required modification of DNAs or nanoparticles (NPs) on the electrodes, which were complicated and time-consuming, extremely limiting their practical application in environmental sample detection. Importantly, most of these electroanalysis methods achieved the detection of As(III), while electrochemical detection of As(V) was rarely developed. Hence, it is still highly desirable to seek a convenient, fast and sensitive electrochemical biosensor for detecting As(V).

Inspiringly, immobilization-free electrochemical biosensing approaches have been intelligently proposed for quantitatively detecting a wide range of analytes, which not only simplified the experimental processes but also circumvented local steric Hindrance.[26–32] Moreover, it is worth noting that the enhanced

College of Chemistry and Pharmaceutical Sciences, Qingdao Agricultural University, Qingdao, 266109, People's Republic of China.
E-mail: lifeng@qau.edu.cn

†Electronic Supplementary Information (ESI) available: Experimental details and supplementary Figures. See DOI: 10.1039/x0xx00000x

View Article Online
DOI: 10.1039/D0CC01821J

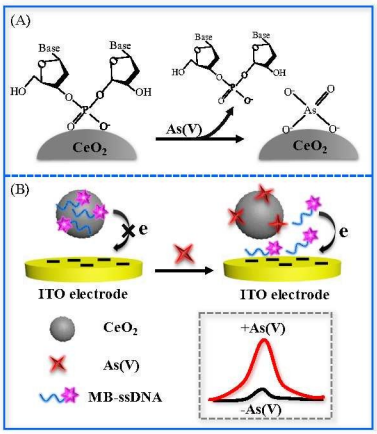

Scheme 1 Scheme illustration of the nanoprobe-based immobilization-free electrochemical strategy for detection of As(V).

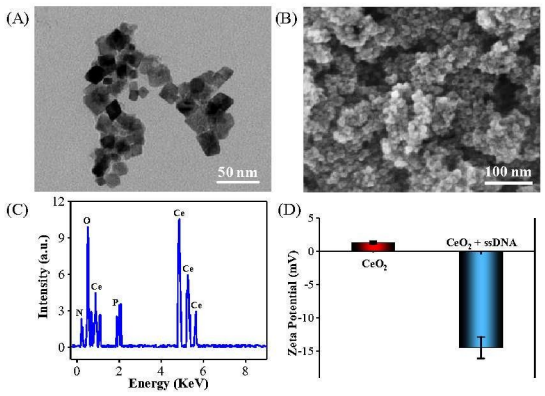

Fig. 1 (A) TEM and (B) SEM images of CeO_2 NPs. (C) EDX characterization of the CeO_2-ssDNA nanocomposite. (D) Zeta potential of CeO_2 NPs before (red bar) and after adsorption (blue bar) of ssDNA.

sensitivity can be achieved because of the improved recognition efficiency in homogeneous solution between the target and recognition unit. Herein, we reported a convenient immobilization-free electrochemical strategy for detecting As(V) with high sensitivity and selectivity based on the ssDNA-functionalized CeO_2 nanoprobe and target-induced displacement reaction. CeO_2 NPs were found to interact with the ssDNA via the phosphate backbone.[33] As(V) has a similar property as phosphate but shows much stronger binding ability toward CeO_2 than phosphate, thus the formed Ce–As(V) coordination complex would release the ssDNA form the CeO_2 surface (Scheme 1A). Therefore, by utilizing this unique property, a facile immobilization-free electrochemical sensing method was constructed for As(V) analysis. The nanoprobe can be fast prepared by mixing CeO_2 NPs with a 5-mer ssDNA labeled with methylene blue (MB-ssDNA). Owing to the relatively low diffusivity, the nanoprobe hardly arrived at the negatively charged indium tin oxide (ITO) electrode, thus causing a small DPV signal. After As(V) being added into the reaction solution, the adsorbed MB-ssDNA would be displaced from the nanoprobe. MB-ssDNA has great diffusion in view of its relatively small size and negative charge, which eventually generated noticeably increased electrochemical signal. Therefore, by taking advantage of the different diffusivity of the MB-ssDNA and the nanoprobe toward the ITO electrode, a facile homogenous electrochemical sensing system for realizing the determination of As(V) was intelligently established. With outstanding virtues of simplicity, rapidness, high specificity, and efficiency, this sensing method successfully achieved As(V) detection in natural water samples, The details of this approach are presented in Scheme 1.

CeO_2 NPs were prepared via a simple hydrothermal method according to the previous report.[34] As shown in Fig. 1 A and B, the size of the as-obtained CeO_2 NPs was about 20.0 ± 3.1 nm by using transmission electron microscopy (TEM) and scanning electron microscopy (SEM). The maximum absorption of the CeO_2 NPs was at 290 nm as revealed by the UV-vis absorption spectrum (Fig. S1, ESI†). Furthermore, the X-ray diffraction pattern (XRD) result showed that the CeO_2 NPs were the typical fluorite cubic structure (Fig. S2, ESI†).[35] Next, the adsorption of ssDNA on CeO_2 was studied. To circumvent the influence of MB molecules, the non-labeled ssDNA displaced MB-ssDNA in this assay. As can be seen from Fig. 1C, Ce, O, N and P elements were clearly detected in CeO_2-ssDNA bioconjugates. Further measurements revealed that the zeta potential of the as-prepared CeO_2 was +1.3 ± 0.2 mV and changed to -14.5 ± 1.6 mV after adsorption ssDNA (Fig. 1D). All the above results confirmed the ssDNA has definitely adsorbed on the surface of CeO_2 NPs.

To explore the feasibility of this homogenous sensing platform for As(V) detection, the DPV signals of the MB-ssDNA in the presence of CeO_2 NPs were first carried out. With the CeO_2 being put to the system, the current signals of the MB-ssDNA sharply diminished with the increasing CeO_2 concentration and leveled off when the concentration of CeO_2 increased to 350 μg/mL (Fig. 2A and B). The obviously decreased current signal was probably that the nanoprobe with low diffusivity hardly reached the ITO electrode surface. At the same time, the MB-ssDNA can be effectively adsorbed by CeO_2 within 2 min and barely changed in the subsequent time (Fig. S3, ESI†), indicating that the as-prepared nanoprobe had outstanding stability and was suitable for establishing a biosensor. In addition, the previous report showed that ssDNA could adsorb on ITO NPs surfaces,[36] thus the possible electrostatic interaction between As(V) and ITO electrode may influence the current signal of MB-ssDNA. The experimental results showed that no obvious change of DPV signal was observed when As(V) was put into the solution containing MB-ssDNA. Next, the feasibility of this sensing method for As(V) detection was investigated. As shown in Fig. 2C, a significant increase of DPV signal was achieved after the addition of As(V) into the system (curve c), demonstrating adsorbed MB-ssDNA was effectively released from the nanoprobe. MB-ssDNA has small size and less negative charge, making it possesses higher diffusivity towards the ITO surface, thus leading to a large DPV signal. More importantly, about 20-fold of the signal-to-background ratio was obtained, indicating that the CeO_2-DNA nanoprobe-based homogeneous electrochemical biosensing could successfully realize As(V) detection.

View Article Online
DOI: 10.1039/D0CC01821J

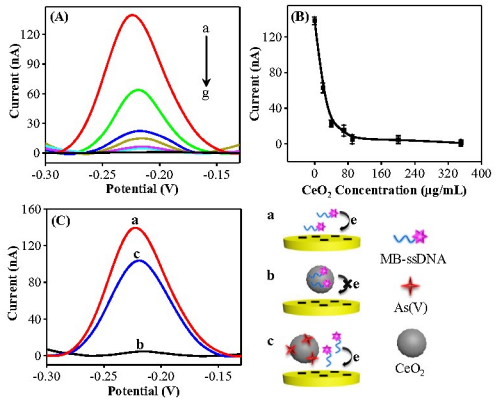

Fig. 2 (A) DPV responses of ssDNA-MB under various concentrations of CeO_2 NPs (from a to g: 0, 20, 40, 70, 90, 200 and 350 μg/mL). (B) DPV peak currents of MB-ssDNA versus different concentrations of CeO_2 NPs. (C) DPV curves of ssDNA-MB under different conditions: (a) MB-ssDNA, (b) MB-ssDNA + CeO_2, (c) MB-ssDNA + CeO_2 + As(V). The concentrations of CeO_2, MB-ssDNA and As(V) were 90 μg/mL, 0.5 μM and 100 μM, respectively. The buffer solution contained 10 mM HEPES, 200 mM NaCl, pH 7.6.

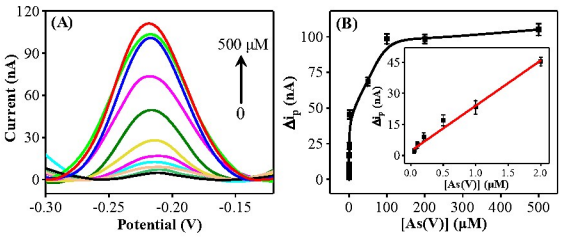

Fig. 3 (A) DPVs of the proposed sensing system toward different As(V) concentrations: 0, 0.05, 0.1, 0.2, 0.5, 1, 2, 50, 100, 200, 500 μM. (B) The DPV peak currents versus different As(V) concentrations. Insets is the calibration plot of DPV peak current against As(V) concentrations. The concentrations of CeO_2 and MB-ssDNA were 90 μg/mL and 0.5 μM, respectively. The buffer solution contained 10 mM HEPES, 200 mM NaCl, pH 7.6. $\Delta i_p = i_p - i_{p,0}$, in which $i_{p,0}$ and i_p are the DPV peak currents in the absence and presence of As(V) with various concentrations, respectively.

To obtain the best electroanalytical performance of the developed method, the amount of the CeO_2 NPs, the salt concentration, the buffer solution pH, and the reaction time were systematically examined. The low concentration of CeO_2 will lead to a high background and excessive concentration of CeO_2 will affect the current signal recovery. Hence, the influence of the CeO_2 NPs concentration was first assessed. In the presence of As(V), the current signal gradually increased with the increasing concentrations of CeO_2 and then decreased when the concentration of CeO_2 reached to 120 μg/mL (Fig. S4, ESI†). The current change Δi_p reached a maximum when the concentration of CeO_2 was 90 μg/mL. Therefore, 90 μg/mL CeO_2 was selected as the optimal concentration. Moreover, Fig. S5 (ESI†) indicated that the highest current response was observed with the concentration of NaCl at 200 mM. Therefore, the best amount of NaCl was 200 mM. Furthermore, the Δi_p increased as pH increased from 5.5 to 8.5 (Fig. S6, ESI†). Taking into the consideration of the application of this system under neutral conditions, pH of 7.6 was adopted in the subsequent experiments. Additionally, Fig. S7 (ESI†) showed that most of the MB-ssDNA reporters were released from the surface of the CeO_2 NPs within 3 min and almost remained constant after 10 min. Such fast signal recovery is beneficial for practical applications. We selected 10 min as the optimal reaction time.

To further demonstrate the ability of the developed homogeneous strategy for sensitive quantifying As(V), the DPV responses of the nanoprobe to As(V) were recorded under the optimal detection conditions. As displayed in Fig. 3, the peak currents progressively enhanced with the increasing As(V) concentrations, revealing that more and more MB-ssDNA molecules were gradually released from the nanoprobe with the increasing amount of As(V), thus resulting in an increase in DPV signals. Fig. 3B showed a pleasurable linear relationship between Δi_p and As(V) concentrations in the range of 50 nM-2 μM and a low detection limit of 20.5 nM for As(V) could be derived based on the 3s/slope method. Furthermore, the repeatability and the reproducibility of the sensing platform were explored. The relative standard deviation (RSD) values were 3.9% and 4.5% respectively, which indicated an acceptable repeatability and reproducibility for this approach. These results confirmed that this electrochemical sensing platform was capable of detecting As(V) with high sensitivity and reliability. More importantly, compared with the currently conventional immobilization-based electrochemical biosensor for arsenic detection, this sensing system effectively circumvented the sophisticated DNA probe or nanomaterials modification processes, making it simple, fast and easy to operate.

Having confirmed the outstanding analytical performance of the sensing system toward As(V), the selectivity was then estimated by testing other possible interfering heavy metal ions and anions. As shown in Fig. 4A and 4B, only As(V) caused a sharply increased current Δi_p, while no obvious change of Δi_p was observed with the interfering substances. Thus, the results demonstrated that the as-proposed biosensing system had remarkable specificity for As(V) over other competing ions. The high specificity can be attributed to the strong Ce-O-As binding force between As(V) and CeO_2, which was higher than the affinities between other ions and CeO_2. In addition, the DPV responses of the sensing system treated with different concentrations of PO_4^{3-} were investigated because PO_4^{3-} might cause the interference. Fig. S8 (ESI†) exhibited that a negligible change of current signal Δi_p was observed when the concentration of PO_4^{3-} was 10 μM and the Δi_p increased to 23.5 nA when the phosphate concentration reached to 100 μM. Since the amount of phosphate in water is very low and it can be easily precipitated by many cations, our method is promising for detecting As(V) in complex real samples.

To further validate the analytical reliability and practical application of the as-proposed method, As(V) quantifications in the environmental samples were tested by employing tap water and lake water. Before performing the real sample test, the water samples were diluted with HEPES buffer. Negligible

View Article Online
DOI: 10.1039/D0CC01821J

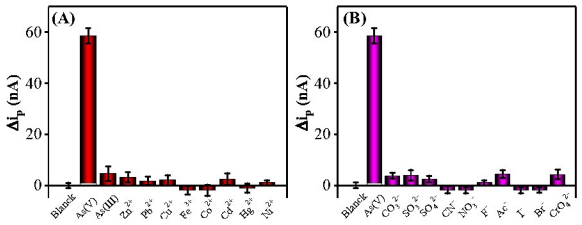

Fig. 4 Specificity of the developed sensing system toward As(V) against other interfering substances. The concentration of As(V) and the other heavy metal ions (A) and anions (B) are 10 μM and 100 μM, respectively. The concentrations of CeO_2 and MB-ssDNA were 90 μg/mL and 0.5 μM, respectively.

changes were detected in those water samples, suggesting that the amount of As(V) was extremely low. Therefore, the recovery tests were carried out by spiking different amount of As(V) into the water samples. The detail results were listed in Table 1. The recovery was ranging from 96% to 105% and the RSD was ranging from 2.7% to 4.1%, which were consistent with the results tested by the ICP-MS method. Taken together, these results confirmed that this homogenous electrochemical platform was capable of analyzing real water samples.

In conclusion, we reported a CeO_2–DNA nanoprobe for immobilization-free electrochemical detection of As(V) based on the competitive coordination effect. By utilizing the diffusivity difference of ssDNA and ssDNA-functionalized CeO_2 nanoprobe toward the electrode, a facile sensing system for the determination of As(V) with high sensitivity and selectivity was intelligently realized. Furthermore, this strategy has successfully achieved the detection of As(V) in natural water samples. More significantly, compared to the common electrochemical As(V) assays, this immobilization-free electrochemical method circumvented the complicated modification and tedious processes, demonstrating the outstanding virtues of simplicity, rapidness, and efficiency. Thus, we anticipate that this facile strategy might open up new opportunity for As(V) determination in the environmental sample analysis.

This work was financially supported by the National Natural Science Foundation of China (Nos. 21804077, and 21775082), Shandong Province Higher Educational Program for Young Innovation Talents, the Major Program of Shandong Province Natural Science Foundation (ZR2018ZC0127), the Special Foundation for Distinguished Taishan Scholar of Shandong Province (ts201511052), and the Research Foundation for Distinguished Scholars of Qingdao Agricultural University (665-1119006).

Conflicts of interest

There are no conflicts to declare

Notes and references

1 H. A. Michael, *Science*, 2013, **341**, 852–853.
2 M. Berg, H. C. Tran, T. C. Nguyen, H. V. Pham, R. Schertenleib and W. Giger, *Enviro. Sci. Technol.*, 2001, **35**, 2621–2626.
3 L. Zhang, X. R. Chen, S. H. Wen, R. P. Liang and J. D. Qiu, *TrAC-Trend. Anal. Chem.*, 2019, **118**, 869–879.
4 R. Gupta, J. S. Gamare, A. K. Pandey, D. Tyagi and J. V. Kamat, *Anal. Chem.*, 2016, **88**, 2459–2465.
5 A. Lopez, Y. Zhang and J. Liu, *J. Colloid Interf. Sci.*, 2017, **493**, 249–256.
6 K. Jomova, Z. Jenisova, M. Feszterova, S. Baros, J. Liska, D. Hudecova, C. J.Rhodes and M. Valko, *J. Appli. Toxicol.*, 2011, 31, 95–107.
7 C. K. Jain and I. Ali, *Water. Res.*, 2000, **34**, 4304–4312.
8 P. Devi, A. Thakur, Y. Lai R., S. Saini, R. Jain and P. Kumar, *TrAC-Trend. Anal. Chem.*, 2019, **110**, 97–115.
9 E. H. Larsen and S. Sturup, *J. Anal. At. Spectrom.*, 1994, **9**, 1099–1105.
10 C. B'hymer and J. A. Caruso, *J. Chromatogr. A*, 2004, **1045**, 1–13.
11 M. Schneider, H. R. Cadorim, B. Welz, E. Carasek and J. Feldmann, *Talanta*, 2018, **188**, 722–728.
12 Y. Cai, *TrAC-Trend. Anal. Chem.*, 2000, **19**, 62–66.
13 B. Liu and J. Liu, *Chem. Commun.*, 2014, **50**, 8568–8570.
14 M. Mulvihill, A. Tao, K. Benjauthrit, J. Arnold and P. Yang, *Ange. Chem. Int. Ed.*, 2008, **47**, 6456–6460.
15 L. Zhang, X. Z. Cheng, L. Kuang, A. Z. Xu, R. P. Liang and J. D. Qiu, *Biosens. Bioelectron.*, 2017, **94**, 701–706.
16 S. H. Wen, X. L. Zhong, Y. D. Wu, R. P. Liang, L. Zhang and J. D. Qiu, *Anal. Chem.*, 2019, **91**, 6487-6497.
17 L. Zeng, D. Zhou, J. Gong, C. Liu and J. Chen, *Anal. Chem.*, 2019, **91**, 1724–1727.
18 L. Tong, X. Wang, W. Gao, Z. Liu, Z. Chen, G. Cheng, W. Cao, M. Sui and B. Tang, *Anal. Chem.*, 2018, **90**, 14507–14513.
19 B. Kou, Y. Chai, Y. Yuan and R. Yuan, *Anal. Chem.*, 2018, **90**, 10701–10706.
20 Z. Guo, M. Yang and X. J. Huang, *Curr. Opin. Electrochem.*, 2017, **3**, 130–136.
21 A. O. Simm, C. E. Banks and R. G. Compton, *Anal. Chem.*, 2004, **76**, 5051–5055.
22 G. Bhanjana, N. Dilbaghi, S. Chaudhary, K. H. Kim and S. Kumar, *Analyst*, 2016, **141**, 4211–4218.
23 S. S. Li, W. Y. Zhou, M. Jiang, Z. Guo, J. H. Liu, L. Zhang and X. J. Huang, *Anal. Chem.*, 2018, **90**, 4569–4577.
24 S. Kempahanumakkagari, A. Deep, K. H. Kim, S. K. Kailasa and H. O. Yoon, *Biosens. Bioelectron.*, 2017, **95**, 106–116.
25 L. Cui, J. Wu and H. Ju, *Biosens. Bioelectron.*, 2016, **79**, 861–865.
26 F. Xuan, T. W. Fan and I. M. Hsing, *ACS Nano*, 2015, **9**, 5027–5033.
27 T. Hou, N. Xu, W. Wang, L. Ge and F. Li, *Anal. Chem.*, 2018, **90**, 9591–9597.
28 X. Yin, T. Hou, B. Huang, L. Yang and F. Li, *Chem. Commun.*, 2019, **55**, 13705–13708.
29 R. Miranda-Castro, D. Marchal, B. Limoges and F. Mavré, *Chem. Commun.*, **2012**, **48**, 8772–8774.
30 F. Xuan, X. Luo and I. M. Hsing, *Anal. Chem.*, 2013, **85**, 4586–4593.
31 J. Chang, X. Wang, J. Wang, H. Li and F. Li, *Anal. Chem.*, 2019, **91**, 3604–3610.
32 J. Zhuang, D. Tang, W. Lai, G. Chen and H. Yang, *Anal. Chem.*, 2014, **86**, 8400–8407.
33 B. Liu, Z. Sun, P. J. Huang and J. Liu, *J. Am. Chem. Soc.*, 2015, **137**, 1290–1295.
34 L. Yang, Y. Ren, W. Pan, Z. Yu, L. Tong, N. Li and B. Tang, *Anal. Chem.*, 2016, **88**, 11886–11891.
35 Z. Ji, X. Wang, H. Zhang, S. Lin, H. Meng, B. Sun, S. George, T. Xia, A. E.Nel and J. I. Zink, *ACS Nano*, 2012, **6**, 5366–5380.
36 B. Liu and J. Liu, *Langmuir*, 2015, **31**, 371–377.

View Article Online
DOI: 10.1039/D0CC01821J

Table of contents

Competitive coordination-based immobilization-free electrochemical biosensor was developed for highly sensitive detection of arsenic(V) using CeO_2–DNA nanoprobe.